

# The Fragile Nature of Road Transportation Systems

Linghang Sun<sup>a,\*</sup>, Yifan Zhang<sup>a</sup>, Cristian Axenie<sup>b</sup>, Margherita Grossi<sup>c</sup>, Anastasios Kouvelas<sup>a</sup>,  
Michail A. Makridis<sup>a</sup>

<sup>a</sup>*Institute for Transport Planning and Systems, ETH Zurich, Zurich, 8093, Switzerland*

<sup>b</sup>*Computer Science Department and Center for Artificial Intelligence, Technische Hochschule  
Nürnberg, Nürnberg, 90489, Germany*

<sup>c</sup>*Intelligent Cloud Technologies Lab, Huawei Munich Research Center, Munich, 80992, Germany*

---

## Abstract

Major cities worldwide experience problems with the performance of their road transportation systems. The continuous increase in traffic demand presents a substantial challenge to the optimal operation of urban road networks and the efficiency of traffic control strategies. Although robust and resilient transportation systems have been extensively researched over the past decades, their performance under an ever-growing traffic demand can still be questionable. The operation of transportation systems is widely believed to display fragile property, i.e., the loss in performance increases exponentially with the linearly increasing magnitude of disruptions, which undermines their continuous operation. The risk engineering community is now embracing the novel concept of (anti-)fragility, which enables systems to learn from historical disruptions and exhibit improved performance as disruption levels reach unprecedented magnitudes. In this study, we demonstrate the fragile nature of road transportation systems when faced with either demand or supply disruptions. First, we conducted a rigorous mathematical analysis to theoretically establish the fragile nature of the systems. Subsequently, by taking into account real-world stochasticity, we implemented a numerical simulation with realistic network data to bridge the gap between the theoretical proof and the real-world operations, to study the impact of uncertainty on the fragile property of the systems. This work aims to help researchers better comprehend the necessity to explicitly consider antifragile design toward the application of future traffic control strategies, coping with constantly growing traffic demand and subsequent traffic accidents.

*Keywords:* (anti-)fragility, road transportation systems, macroscopic fundamental diagram, model stochasticity

---

## 1. Introduction

As reported by both the U.S. Department of Transportation (2019) and Federal Statistical Office of Switzerland (2020), motorized road traffic before the pandemic has experienced an approximate 50% growth over the past few decades. Researchers have also found that the continuous growth in traffic volume has consequently contributed to a rise in disruptive events, such as severe congestion and more frequent accidents (Chang and Xiang, 2003). As motorized individual traffic has been demonstrated with real data to recover from the pandemic (Büchel

---

\*Corresponding author.

*Email address:* [lisun@ethz.ch](mailto:lisun@ethz.ch) (Linghang Sun)

et al., 2022; Ciuffini et al., 2023), it is anticipated to persist in such increase in the coming decades (Zhang and Zhang, 2021).

Meanwhile, there is a common understanding that road transportation networks can exhibit fragile properties. Fragility signifies a system’s susceptibility to exponentially escalating performance deterioration as disruptions increase in magnitude. One prominent example is the BPR function (U.S. Bureau of Public Roads, 1964), with empirical data at the link level, distinctly illustrates that travel time grows exponentially with traffic flow, leading to an infinite temporal cost when the traffic influx is at the maximal density of the network. Moreover, not limited to road transportation systems, most types of transportation systems also display similar fragile characteristics, such as railway systems (Saidi et al., 2023) and aviation systems (U.S. Congress, Office of Technology Assessment, 1984).

Researchers have devoted extensive efforts to designing robust and resilient transportation systems (Shang et al., 2022; Mattsson and Jenelius, 2015). However, when accounting for the ever-growing traffic volume in urban road networks and the exponentially escalating adversarial consequences, it is natural for us to wonder whether the current level of robustness and resilience can still guarantee the performance of road networks considering a long-term time horizon. Hence, we introduce the cutting-edge concept of (anti-)fragility to explain the phenomenon that roadside performance deteriorates exponentially with linearly growing disruptions. Previous studies discussing this fragile phenomenon have primarily relied on intuitive reasoning and empirical data rather than rigorous mathematical analysis. This paper serves as a proof of concept, aiming to establish the fragile nature of road transportation systems through mathematical analysis. Additionally, as stochasticity prevails in transportation systems in the real world, we designed a numerical simulation considering real-world stochasticity to study to what extent such realistic uncertainties can influence the fragile characteristics of transportation systems. The overarching objective is to provide insights to transportation researchers for the future design of transportation systems and control strategies to be not only robust and resilient but also antifragile.

The remainder of this paper is structured as follows. Section 2 introduces (anti-)fragility and reviews specific traffic-related mathematical models. Section 3 formulates the mathematical meaning of (anti-)fragility and its applications. Then we conduct the mathematical proof in Section 4, whereas Section 5 presents the numerical simulation with real-world stochasticity. With Section 6, we conclude the fragile nature and its implications for future studies.

## 2. Literature review

Various terminologies have been proposed to evaluate the performance of transportation systems and two commonly used terms to characterize the extent of performance variations under stress are robustness (Duan and Lu, 2014) and resilience (Calvert and Snelder, 2018). However, the definitions of robustness and resilience can vary under different contexts, even within the transportation domain, due to different backgrounds and points of view of the authors (Corman et al., 2018), and sometimes even used interchangeably (Corman et al., 2018). In this study, we adopt the principle proposed in Zhou et al. (2019), wherein robustness involves evaluating a system’s ability to maintain its initial state and withstand performance degradation when confronted with uncertainties and disturbances. On the other hand, resilience emphasizes a system’s capability and promptness in recovering from major disruptions and returning to its original state. In brief, robustness relates to resistance, whereas resilience is about recovery.

Nevertheless, these two terms can overlook the consideration of a longer timespan and the potential escalation of disruptions, which is particularly relevant in the context of transportation.

Thus, there is the necessity to introduce a new concept to address this gap. The concept of antifragility was initially proposed by Taleb (2012) and mathematically elaborated in Taleb and Douady (2013), and it serves as a general concept aimed at transforming people’s understanding and perception of risk. By embracing current risks, we can potentially leverage and adapt to future risks with larger magnitudes. On the other hand, Ever since being proposed, antifragility has gained popularity in the risk engineering community across multiple disciplines, such as economy (Manso et al., 2020), biology (Kim et al., 2020), medicine (Axenie et al., 2022), energy (Coppitters and Contino, 2023), and robotics (Axenie and Saveriano, 2023). Generally speaking, when the performance of a system is compromised due to unexpected disruptions, the relationship between the loss in performance and the magnitude of the disruptions would be convex for a fragile system, while being concave for an antifragile system.

In transportation, by unveiling the convex relationship between travel time and traffic flow with empirical data, the BPR function (U.S. Bureau of Public Roads, 1964), as shown in Eq. 1 gives an intuitive example showing the fragility of the transportation systems on a link level. However, to uphold the statement that road transportation systems are fragile, an empirical function like BPR alone is not sufficient without rigid mathematical proof. Also, it is desired to show the fragility not only on the link level but also on the macroscopic level, as well as for different types of disruption.

$$T = T_{ff} \left( 1 + \alpha \left( \frac{q}{q_{\max}} \right)^\beta \right) \quad (1)$$

Prior to diving into the demonstration of the fragile characteristics of road transportation systems, various traffic-related models should first be explained. The assessment of traffic performance can be conducted at either the microscopic or macroscopic level. However, due to the non-identical properties of traffic across these levels, researchers have formulated diverse traffic models to offer a more precise description of traffic dynamics at different levels. These models serve the purpose of accurately portraying traffic behavior, with some being derived numerically from data, while others are developed through analytical methods.

Although various traffic models on the microscopic level have been proposed, we select two most representative models, one numerical and one analytical, as examples. The earliest study on traffic performance was carried out and described in Greenshields et al. (1934) on a section of a highway and created the first Fundamental Diagram (FD), as shown in Fig. 1(a), which exhibits the relationship between traffic flow, denoted as  $q$ , and density, denoted as  $k$ , in the shape of a second-degree polynomial. Later, other researchers also developed FDs in various forms, with the most commonly applied FD being proposed in Daganzo (1994), as shown in Fig. 1(b), and is characterized by two linear functions. While the Greenshields FD is entirely generated through the fitting of the polynomial coefficients, the Daganzo FD, on the other hand, is derived analytically and incorporates variables with physical meanings, i.e., the free-flow speed, back-propagation speed, and critical density, denoted as  $v_f$ ,  $w$ , and  $k_c$ , respectively.

On the macroscopic level, a Macroscopic Fundamental Diagram (MFD) can be produced by aggregating data points gathered from each single link within this network. Similar to FD, MFD can be represented through different models, and the most representative and widely applied approaches include polynomials and multi-regime linear functions. Daganzo and Geroliminis (2008) is the first study to ever analytically generate an MFD by using the Method of Cuts (MoC). This analytical method demonstrated the feasibility of using variables with physical

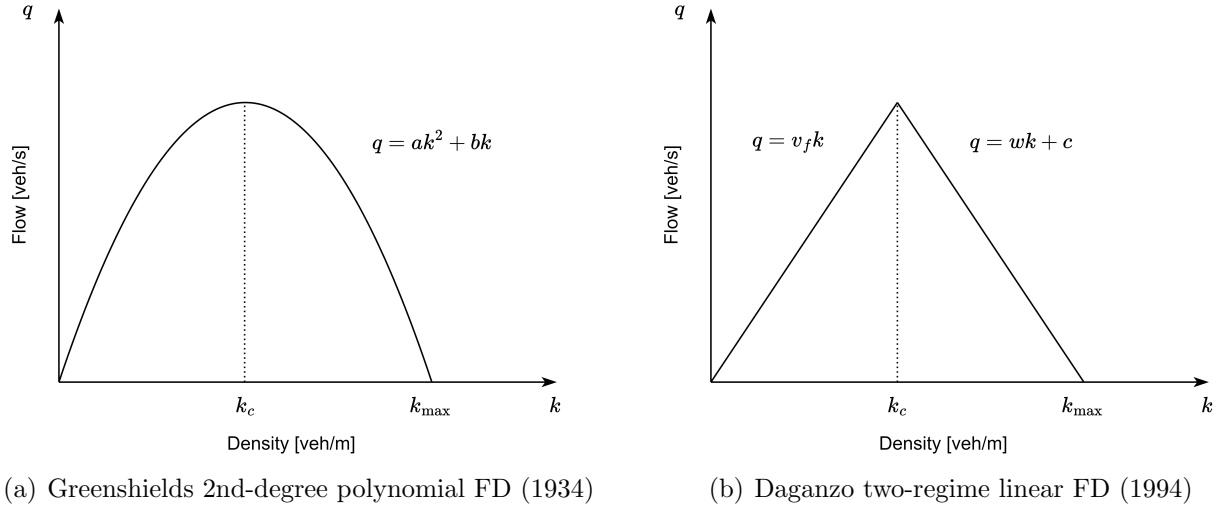


Figure 1: Mathematical models of FDs

meanings to approximate an MFD with multi-regime linear functions in a homogenous region, as shown in Fig. 2(b). Leclercq and Geroliminis (2013) modified the original MoC to accommodate topology and signal timing heterogeneity within the network. Although theoretically an infinite number of cuts can be generated to approximate the MFD, only the practical cuts, the solid lines in Fig. 2(b), are used for simplicity reasons.

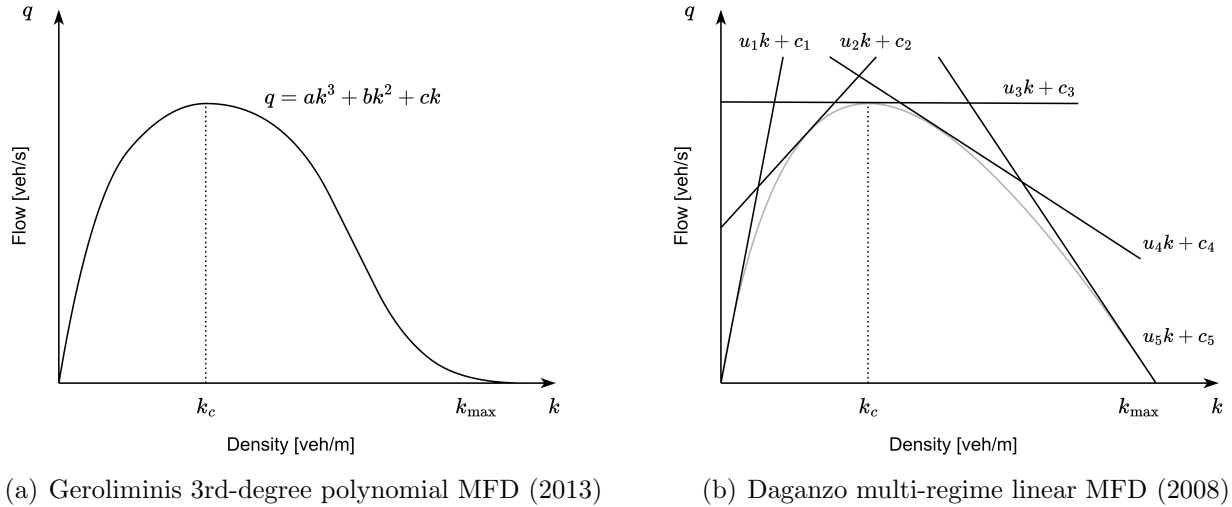


Figure 2: Mathematical models of MFDs

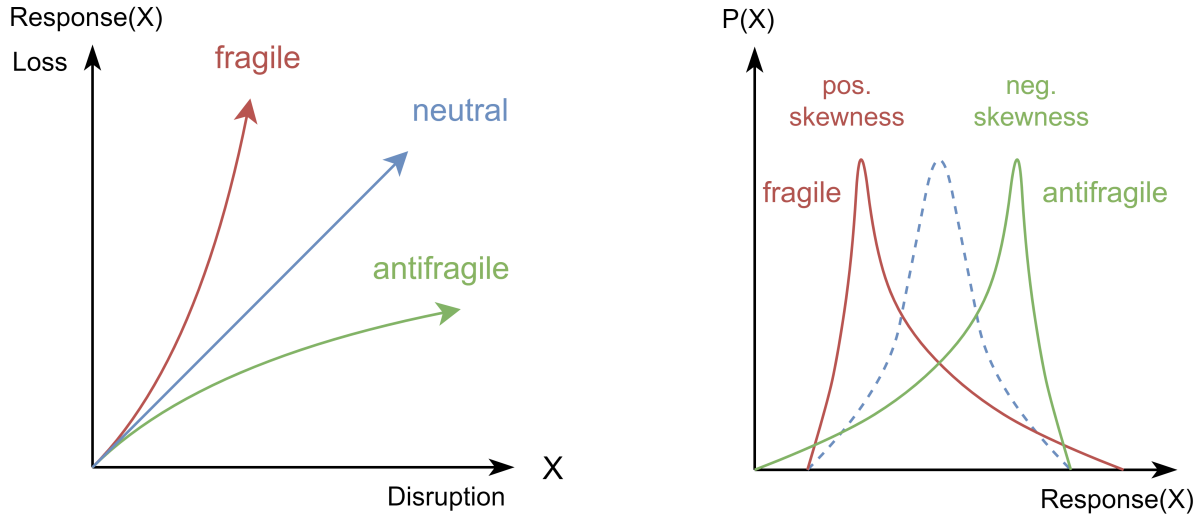
As also acknowledged in these works, some variables, particularly the parameters related to signalization, are hard to acquire in the real world with actuated signals. Therefore, simplified MFDs are also widely adopted when solving more applicational problems like traffic control. Daganzo et al. (2018) approximated a simplified MoC-based MFD using only three cuts from one of each stationary, forward, and backward observer, and formed the uMFD. Other researchers also approximated the MFDs based on collected data with polynomials, e.g., a third-degree polynomial in Geroliminis et al. (2013) as shown in Fig. 2(a). It should be noted that since the

data points near the maximal density are scarce overall, the approximated MFDs are sometimes not strictly realistic. For example, the third-degree polynomial in Geroliminis et al. (2013) has only one real root, indicating the speed is above zero despite that the network has reached its maximal density and formed a gridlock. As claimed in Daganzo and Geroliminis (2008), since MFD should be concave, the flow and speed are both zero by definition at maximal density.

### 3. Problem formulation

As explained in Section 2, an (anti-)fragile response of a system can be characterized through a nonlinear relationship between the performance loss and the magnitude of the disruption, as shown in Fig. 3(a). Both nonlinear functions can be represented by Jensen’s inequality (Jensen, 1906), with either  $E[g(X)] \geq g(E[X])$  for a fragile response or  $E[g(X)] \leq g(E[X])$  for an antifragile response. This relationship can then be determined through the second derivative (Ruel et al., 1999), i.e., a positive second derivative featuring a convex function and hence a fragile system. It should be noted that the calculation of the derivatives is only possible when the function is continuous and differentiable, which means the underlying mathematical model should be present.

However, in most real-world scenarios, the mathematical function of the system is unknown, and only discrete measurements of the system’s performance are available. In this case, we can calculate the distribution skewness to determine the (anti-)fragile property of the system, as illustrated with an example of financial deficit in Taleb and Douady (2013) and Coppitters and Contino (2023) when designing an antifragile renewable energy system. A negative skewness represents the long tail points left and indicates an antifragile response, as shown in Figure 3(b).



(a) Nonlinear relationship for a continuous function      (b) Distribution skewness for discrete measurements

Figure 3: Characteristics and identification of (anti-)fragility

In this paper, we address three sets of opposing concepts when studying the fragile nature of road transportation systems:

- microscopic / macroscopic
- demand disruption / supply disruption

- onset of disruption / recovery from disruption

As microscopic and macroscopic traffic models were introduced in Section 2, in this section, we initiate the discussion by differentiating between demand and supply disruptions, with the latter also sometimes referred to as MFD disruptions. As traffic networks primarily involve the management of supply and demand, we consider that any traffic disruption in the real world can be classified as either a demand or a supply disruption. A demand disruption can be easily understood as, for example, surging traffic due to a social event, whereas a supply disruption may indicate an impaired network performance due to external factors, such as adversarial weather or lane closure. Additionally, since disruptions represent abnormal cases that only exist temporarily, we consider not only the onset of disruptions but also assess the recovery process of the systems following such disruptions. The scheme of onset and recovery from either demand or supply disruptions are illustrated in Figure 4(a) and Figure. 4(b) on the macroscopic level. Since FDs share similar profiles as MFDs, we use MFDs here as examples for illustration. We denote the FD/MFD profile as  $G(k)$  and assume a constant base demand in the network as  $q$ . The initial density corresponding to the base demand, critical density, the new density after disruption, and the gridlock density are denoted as  $k_0$ ,  $k_c$ ,  $k'$ , and  $k_{\max}$ , respectively. For supply disruption, we introduce a disruption magnitude coefficient  $r$  so that the disrupted MFD profile can be represented as  $(1-r)G(k)$ . It should also be noted that on the network level, instead of traffic flow - density, MFD can also be represented with vehicle accumulation - trip completion, such as in Zhou and Gayah (2021); Kouvelas et al. (2017); Genser and Kouvelas (2022). Hence, with vehicle accumulation denoted as  $n$ ,  $G(k)$  and  $k_*$  can also be replaced with  $G(n)$  and  $n_*$ .

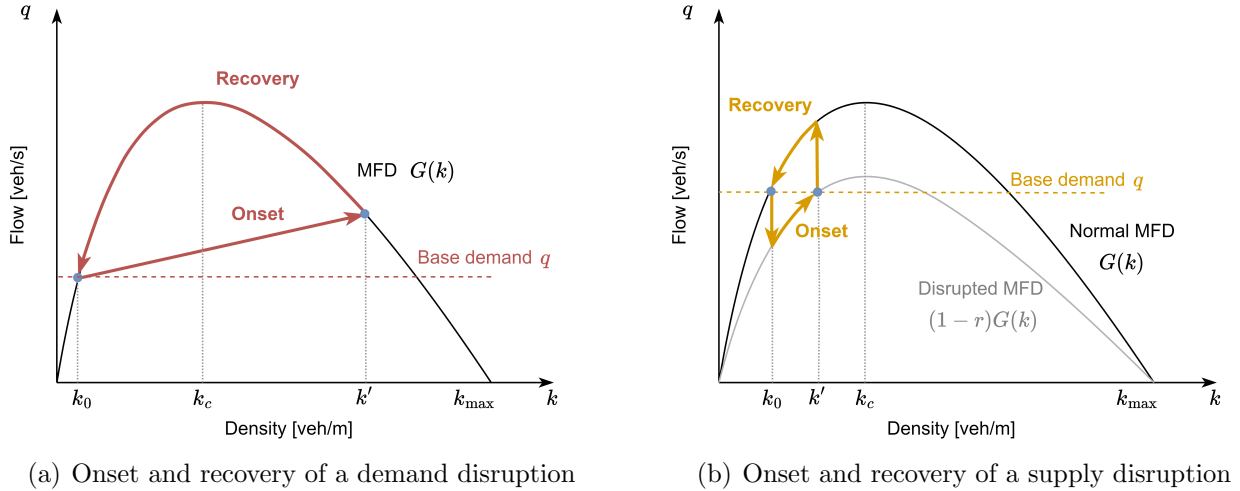


Figure 4: Onset and recovery of disruptions

As the study of (anti-)fragility also involves the recovery process following a potential disruption, several assumptions need to be established to define the scope of our study. A critical condition to avoid is the network succumbing to a complete gridlock, where recovery is not possible anymore.

1. For demand disruptions,  $k' > k_c$ , whereas for supply disruptions,  $k' < k_c$ .

A surging demand is considered a disruption only when its presence leads to a reduction in the network's serviceability, i.e., causing the traffic state to enter the congested zone of

the MFD. On the other hand, for supply disruption with the constant base demand, if the traffic state can ever surpass the maximal capacity of the disrupted MFD profile, then the density will continue to accumulate until the network reaches gridlock, as the incoming flow is greater than the maximal possible outgoing flow.

2. For demand disruptions,  $q < G(k')$ , whereas for supply disruptions,  $q < (1 - r)G(k_c)$ .

Likewise, the necessity of this assumption also lies in the avoidance of gridlock for both demand and supply disruptions. If the base demand is higher than the outgoing flow after a demand disruption or the maximal flow after a supply disruption, then the traffic state will continue to move to complete gridlock.

3. The onset of the disruptions can happen instantaneously, while the recovery from disruptions is a gradual process.

This can be particularly true for demand disruptions characterized by a rapid influx of traffic into the network. Therefore, it can be understood as a sudden change from one stable traffic state to another stable state. On the other hand, the recovery from disruptions can take significantly longer and thus it is a traffic unloading and congestion dissipation process instead of an instantaneous event.

#### 4. Mathematical proof of the fragility of road transportation systems

In this section, we conduct mathematical proof to demonstrate the fragile nature of the transportation systems on both the microscopic and the macroscopic levels. We summarize in Table 1 the structure of this section to prove mathematically the fragile nature of road transportation networks. In the following study, the indicator for the network performance to study the instantaneous disruption onset and between different stable states is the Average Time Spent (ATS), as ATS is the same for each vehicle that entered the network. On the other hand, for the study of the disruption recovery, we use Total Time Spent (TTS), as applied in Zhou and Gayah (2021); Chen et al. (2022); Rodrigues and Azevedo (2019), to better reflect the temporal costs for all the vehicles in this process, as the time spent in the network for different vehicles varies distinctively.

Table 1: Structure of the mathematical proof

Disruption	Demand		Supply	
	Micro	Macro	Micro	Macro
Onset	Section 4.1.1 Proposition 1	Section 4.1.2 Proposition 2	Section 4.2.1 Proposition 4	Section 4.1.2 Proposition 5
Recovery	-	Section 4.1.3 Proposition 3	-	Section 4.2.3 Proposition 6

##### 4.1. Demand disruption

As outlined in Section 2, the presence of a positive second derivative in performance loss concerning the extent of disruption serves as an indication of the transportation system's fragility. To illustrate the system's fragility to demand disruption, we analyze the derivatives of time

spent relative to the initial disruption demand, either represented by disruption density  $k'$ , or disruption vehicle accumulation  $n'$ . If the system is neither fragile nor antifragile, this measure is expected to exhibit linear growth alongside the disruption. Quoting and in line with the famous statistician George Box, "All models are wrong, but some are useful.", we employ both numerical and analytical traffic models to investigate the fragile property under the onset of demand disruption at both microscopic and macroscopic scales.

#### 4.1.1. Onset of demand disruption on the microscopic level

To prove mathematically that transportation systems are fragile on the microscopic level with stable traffic states, we choose the second-degree polynomial FD in Greenshields et al. (1934) as the numerical mathematical model and the two-regime linear FD Daganzo (1994) as the analytical mathematical model.

**Proposition 1.** *Road transportation systems are fragile with the onset of demand disruptions on the microscopic level.*

*Proof.* For the Greenshields second-degree polynomial FD, the following equations describe traffic in a stable state. The traffic flow, density, and speed are denoted as  $q$ ,  $k$ , and  $v$  respectively, while  $a$  and  $b$  are polynomial coefficients. Then the traffic flow  $q$  and average speed  $v$  can be determined as in Eq. 2 and Eq. 3, with the speed-density profile shown in Fig. 5(a).

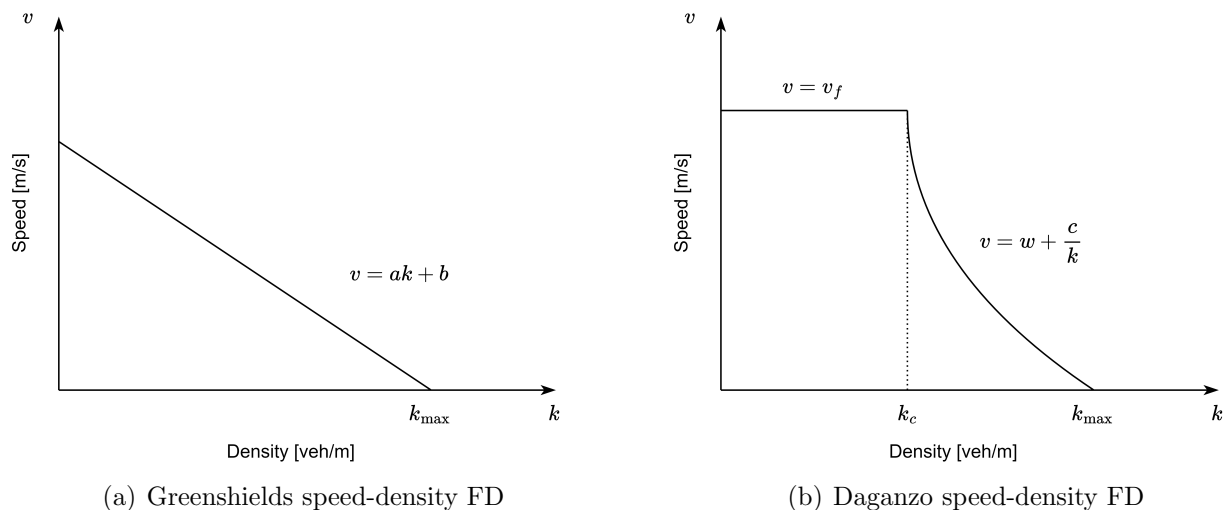


Figure 5: Mathematical models of speed-density FDs

$$G(k) = ak^2 + bk \tag{2}$$

$$v(k) = \frac{q}{k} = ak + b \tag{3}$$

With the sudden onset of a demand disruption with a traffic density of  $k'$ . For a link with a given length of  $L$ , the ATS and its first and second derivatives over such disruption density  $k'$  are:

$$ATS = \frac{L}{v(k')} = \frac{L}{ak' + b} \quad (4)$$

$$\frac{dATS}{dk'} = -aL(ak' + b)^{-2} \quad (5)$$

$$\frac{d^2ATS}{dk'^2} = 2a^2L(ak' + b)^{-3} \quad (6)$$

Since the physical meaning of the term  $ak' + b$  is the average speed of vehicles on this link and should always be a non-negative value while  $a$  is negative, thus, both the first and second derivatives of ATS over  $k'$  are positive, indicating the fragility of transportation systems on a microscopic level.

In this Daganzo two-regime linear model, the speed-density FD can be formulated as the following Eq. 7, as shown in Fig. 5(b).

$$v(k) = \begin{cases} v_f, & 0 \leq k < k_c \\ w + \frac{c}{k}, & k_c \leq k \leq k_{\max} \end{cases} \quad (7)$$

When the disruption density  $k'$  is below the critical density  $k_c$ , the ATS and its first and second derivatives are:

$$ATS = \frac{L}{v_f} \quad (8)$$

$$\frac{dATS}{dk'} = 0 \quad (9)$$

$$\frac{d^2ATS}{dk'^2} = 0 \quad (10)$$

The second derivative being zero indicates the traffic states before  $k_c$  are neither fragile nor antifragile. As per Assumption 1, the congested area of the MFD is the study focus for demand disruptions. And when the density is over  $k_c$ , the ATS and its derivatives are:

$$ATS = \frac{L}{v(k')} = \frac{L}{w + \frac{c}{k'}} \quad (11)$$

$$\frac{dATS}{dk'} = \frac{cL}{(wk' + c)^2} \quad (12)$$

$$\frac{d^2ATS}{dk'^2} = \frac{-2wcL}{(wk' + c)^3} \quad (13)$$

Before the disruption density  $k'$  reaches the maximal density  $k_{\max}$  of this link,  $wk' + c > 0$  always holds true, and since  $w < 0$  as well as  $c > 0$ , therefore, both the first and second derivatives are positive. □

#### 4.1.2. Onset of demand disruption on the macroscopic level

Likewise, on the macroscopic level, we study the fragile property based on the third-degree polynomial MFD in Geroliminis et al. (2013) and multi-regime linear MFD based on MoC in Daganzo and Geroliminis (2008).

**Proposition 2.** *Road transportation systems are fragile with the onset of demand disruptions on the macroscopic level.*

*Proof.* For MFD approximated with a third-degree polynomial, similar to the Greenshields FD in Eq. 2, we have:

$$G(k) = ak^3 + bk^2 + ck \quad (14)$$

$$v(k) = \frac{q}{k} = ak^2 + bk + c \quad (15)$$

Consequently, the ATS and its first and second derivatives are:

$$ATS = \frac{L}{v(k')} = \frac{L}{ak'^2 + bk' + c} \quad (16)$$

$$\frac{dATS}{dk'} = \frac{-(2ak' + b)L}{(ak'^2 + bk' + c)^2} \quad (17)$$

$$\frac{d^2ATS}{dk'^2} = \frac{\frac{3}{2}(2ak' + b)^2 + \frac{1}{2}(b^2 - 4ac)}{(ak'^2 + bk' + c)^3}L \quad (18)$$

As it should be assumed that Eq. 15 should have real roots, indicating the speed as the root of this second-degree polynomial ought to be a real number, so  $b^2 - 4ac > 0$  should also hold true. Therefore, the second derivative is always positive.

In MoC, the MFD can be approximated by a series of linear functions. In a similar manner to the Daganzo two-regime linear FD, for any linear function, as in Eq. 13, the second derivative of ATS over density  $k$  is defined as:

$$\frac{d^2ATS}{dk'^2} = \frac{-2u_i c_i L}{(u_i k' + c_i)^3} \quad (19)$$

Therefore, as  $c_i$  is positive for any cut since the y-intercept should be positive, whether the second derivative is positive or negative depends only on  $u_i$ . Now We group these cuts based on the value of  $u_i$ , and the cuts that intercept the MFD before the critical density  $k_c$  belong to one group (blue,  $u_i > 0$ , as shown in Fig. 6) while the others with intercepts larger than the critical density  $k_c$  belong to the other group (red,  $u_i < 0$ ), with an exception in case there's a cut at the critical density (gray,  $u_i = 0$ ). Therefore, when the traffic states exceed the critical density, which conforms to Assumption 1, the transportation systems show a fragile property.  $\square$

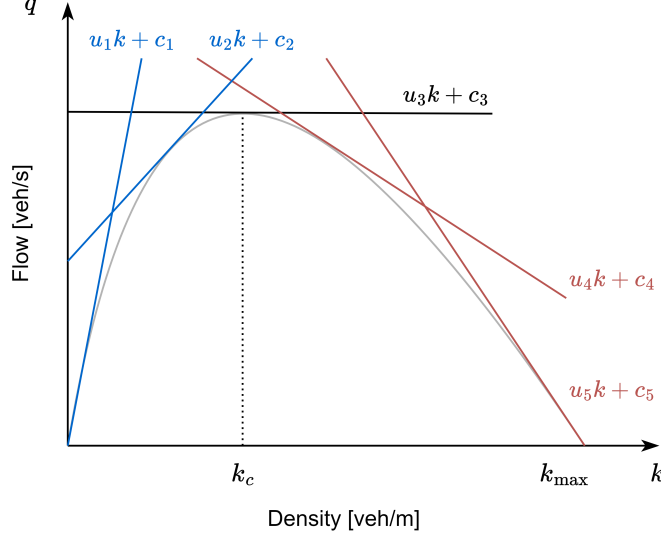


Figure 6: Daganzo multi-regime linear MFD

#### 4.1.3. Recovery from demand disruption

On the macroscopic level, we study the performance of a road network considering an initial demand as a disruption as well as the capability of this network to absorb and dissipate disruption. Although in real-world cases, a surging traffic demand often lasts over a short period following a certain distribution, for simplicity reasons, we consider this demand as a disruption that happens instantly in the network, which is denoted as  $n'$  at time  $t' = 0$ .

Since the MoC is based on a series of linear functions with decreasing gradients as the vehicle accumulation increases, the complete MoC can be represented into multiple sets of consecutive duo linear functions as Figure 7 shows. The four constants  $a_1$ ,  $a_2$ ,  $b_1$ , and  $b_2$  are the slope and y-intercept on the coordinates. While  $b_1 > b_2 > 0$  and are both non-negative values, whether each of  $a_1$  and  $a_2$  is positive or negative is yet uncertain. We refer to these two linear functions as the more congested branch and the less congested branch. Here, the critical accumulation  $n_c$  does not represent the critical point of the entire MFD, but rather the critical accumulation of any consecutive pair of cuts. After a certain period  $t_c$ , the number of vehicles in the network reaches this critical accumulation  $n_c$ . After any period  $t > t_c$ , the vehicle accumulation becomes  $n$ . We also denote the initial trip completion and critical trip completion as  $m_0 = a_1 n' + b_1$  and  $m_c = a_1 n_c + b_1$  respectively.

**Proposition 3.** *Road transportation systems are fragile when going through the recovery process from demand disruptions.*

*Proof.* The duo linear functions representing every two consecutive cuts of the MFD can be formulated into the following Eq. 20, with  $a_2 > a_1$  and  $b_1 > b_2$ :

$$G(n) = \begin{cases} a_1 n + b_1, & n_c \leq n < n_{\max} \\ a_2 n + b_2, & 0 \leq n < n_c \end{cases} \quad (20)$$

The system dynamics can be summarized as the following Eq. 21.

$$\frac{dn}{dt} = -G(n) + q = -a_i n - b_i + q \quad (21)$$

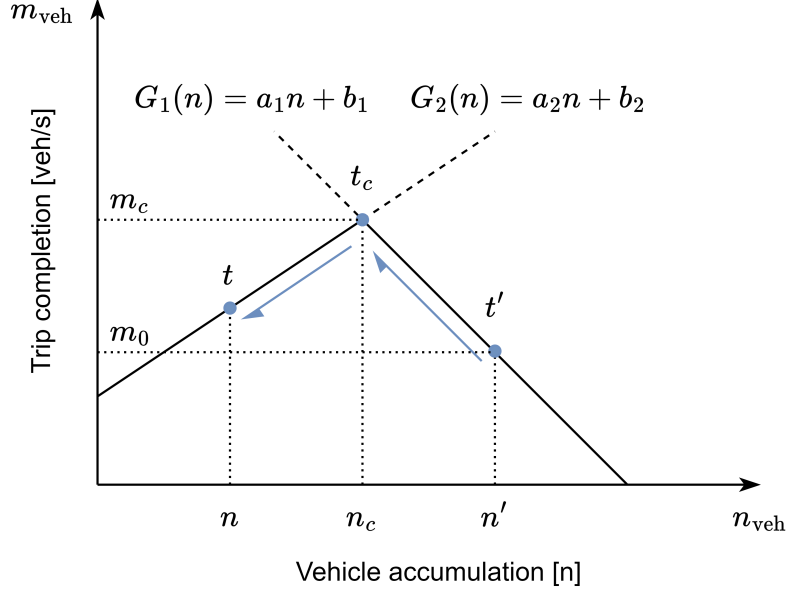


Figure 7: Simplification of MoC

Therefore, if the traffic states stay only on a specific branch, and when given any initial vehicle accumulation  $n_1$  at the beginning of a period from  $t_1$  to  $t_2$ , the number of vehicles  $n_2$  at the end of this period can be determined through a definite integral:

$$\int_{t_1}^{t_2} dt = - \int_{n_1}^{n_2} \frac{1}{a_i n + b_i - q} dn \quad (22)$$

$$t_2 - t_1 = -\frac{1}{a_i} \ln \left( \frac{a_i n_2 + b_i - q}{a_i n_1 + b_i - q} \right) \quad (23)$$

$$n_2 = \frac{e^{-a_i(t_2-t_1)}(a_i n_1 + b_i - q)}{a_i} - \frac{b_i - q}{a_i} \quad (24)$$

Here we consider the initial vehicle accumulation after the occurrence of disruption  $n'$  at the more congested branch and assume after any time  $t$ , the traffic state is still on the same branch. Then the vehicle accumulation  $n$  at any given time  $t$  would be:

$$n = \frac{a_1 n' + b_1 - q}{a_1} e^{-a_1 t} - \frac{b_1 - q}{a_1} \quad (25)$$

The TTS can be calculated as the definite integral over this period  $t$ :

$$TTS = \int_0^t n dt = \int_0^t \left( \frac{a_1 n' + b_1 - q}{a_1} e^{-a_1 t} - \frac{b_1 - q}{a_1} \right) dt \quad (26)$$

$$= -\frac{a_1 n' + b_1 - q}{a_1^2} e^{-a_1 t} - \frac{b_1 - q}{a_1} t + \frac{a_1 n' + b_1 - q}{a_1^2} \quad (27)$$

Now we calculate the derivative of TTS over  $n'$  with  $t$  fixed as a constant parameter.

$$\frac{dTTS}{dn'} = \frac{1}{a_1} - \frac{e^{-a_1 t}}{a_1} \quad (28)$$

$$\frac{d^2TTS}{dn'^2} = 0 \quad (29)$$

The second derivative of TTS over  $n'$  is 0, indicating that when the traffic states change only on a single branch, it shows neither fragility nor antifragility.

On the other hand, when the traffic state goes over the critical vehicle accumulation  $n_c$ , meaning it moves from the more congested branch into the less congested branch, the property of fragility or antifragility may be different. As the MFD is a piecewise function, we calculate the TTS separately on both the more and the less congested branches, denoted as  $TTS_1$  and  $TTS_2$ . Since the critical time  $t_c$  is still unknown, we need to determine  $t_c$  first, similar to Eq. 23.

$$t_c = -\frac{1}{a_1} \ln \left( \frac{a_1 n_c + b_1 - q}{a_1 n' + b_1 - q} \right) \quad (30)$$

As both  $a_1 n_c + b_1$  and  $a_2 n_c + b_2$  are equal to  $m_c$ , we can rewrite the above Eq. 30 as:

$$t_c = -\frac{1}{a_1} \ln \left( \frac{m_c - q}{a_1 n' + b_1 - q} \right) \quad (31)$$

Likewise to Eq. 27, the  $TTS_1$  for the more congested branch is:

$$TTS_1 = -\frac{a_1 n' + b_1 - q}{a_1^2} e^{-a_1 t_c} - \frac{b_1 - q}{a_1} t_c + \frac{a_1 n' + b_1 - q}{a_1^2} \quad (32)$$

$$= -\frac{m_c - q}{a_1^2} + \frac{b_1 - q}{a_1^2} \ln \left( \frac{m_c - q}{a_1 n' + b_1 - q} \right) + \frac{a_1 n' + b_1 - q}{a_1^2} \quad (33)$$

Since TTS is the sum of both  $TTS_1$  and  $TTS_2$  each on the more congested and the less congested branches, the second derivative of TTS would also be the sum of the derivatives of  $TTS_1$  and  $TTS_2$ . The first and second derivatives of  $TTS_1$  are:

$$\frac{dTTS_1}{dn'} = -\frac{b_1 - q}{a_1} (a_1 n' + b_1 - q)^{-1} + \frac{1}{a_1} \quad (34)$$

$$\frac{d^2TTS_1}{dn'^2} = (b_1 - q) (a_1 n' + b_1 - q)^{-2} \quad (35)$$

For the vehicle accumulation on the less congested branch from  $t_c$  to any given time  $t$ , according to Eq. 24, we have:

$$n = \frac{e^{-a_2(t-t_c)}(a_2 n_c + b_2 - q)}{a_2} - \frac{b_2 - q}{a_2} \quad (36)$$

$$= \frac{e^{a_2 t_c} (m_c - q)}{a_2} e^{-a_2 t} - \frac{b_2 - q}{a_2} \quad (37)$$

The  $TTS_2$  for the less congested branch would be:

$$TTS_2 = \int_{t_c}^t n dt = \int_{t_c}^t \left( \frac{e^{a_2 t_c} (m_c - q)}{a_2} e^{-a_2 t} - \frac{b_2 - q}{a_2} \right) dt \quad (38)$$

$$= -\frac{e^{-a_2 t} (m_c - q)}{a_2^2} e^{a_2 t_c} + \frac{b_2 - q}{a_2} t_c + \frac{m_c - q}{a_2^2} - \frac{b_2 - q}{a_2} t \quad (39)$$

The derivatives on the less congested branch are:

$$\frac{dTTS_2}{dn'} = -\frac{(m_c - q)^{1 - \frac{a_2}{a_1}} e^{-a_2 t}}{a_2} (a_1 n' + b_1 - q)^{\frac{a_2}{a_1} - 1} + \frac{b_2 - q}{a_2} (a_1 n' + b_1 - q)^{-1} \quad (40)$$

$$\frac{d^2 TTS_2}{dn'^2} = -\left( \frac{(a_2 - a_1)(m_c - q)^{1 - \frac{a_2}{a_1}} e^{-a_2 t}}{a_2} (a_1 n' + b_1 - q)^{\frac{a_2}{a_1}} + \frac{a_1(b_2 - q)}{a_2} \right) (a_1 n' + b_1 - q)^{-2} \quad (41)$$

According to Assumption 2, we have  $m_0 - q > 0$ . The second derivative of the whole congestion dissipation process from the more congested branch to the less congested branch would be:

$$\frac{d^2 TTS}{dn'^2} = \frac{d^2 TTS_1}{dn'^2} + \frac{d^2 TTS_2}{dn'^2} \quad (42)$$

$$= \left( b_1 - q - \frac{e^{-a_2 t}}{a_2} (a_2 - a_1)(m_c - q)^{1 - \frac{a_2}{a_1}} (m_0 - q)^{\frac{a_2}{a_1}} - \frac{a_1(b_2 - q)}{a_2} \right) (m_0 - q)^{-2} \quad (43)$$

Since  $m_0 - q > 0$ , and if a transportation system is to be fragile,  $\frac{d^2 TTS}{dn'^2}$  should also be positive, and the following equation has to be true:

$$b_1 - q - \frac{e^{-a_2 t}}{a_2} (a_2 - a_1)(m_c - q)^{1 - \frac{a_2}{a_1}} (m_0 - q)^{\frac{a_2}{a_1}} - \frac{a_1(b_2 - q)}{a_2} > 0 \quad (44)$$

Since it is assumed that the traffic state transits from the more congested branch into the less congested branch, we have  $t > t_c$  and  $a_2 > a_1$ . Therefore, regardless of whether  $a_2$  is positive or negative, the following relationship always holds:

$$-\frac{e^{-a_2 t}}{a_2} > -\frac{e^{-a_2 t_c}}{a_2} \quad (45)$$

As the following three terms,  $a_2 - a_1$ ,  $(m_c - q)^{1 - \frac{a_2}{a_1}}$ , and  $(m_0 - q)^{\frac{a_2}{a_1}}$  are all positive, the following relationship always holds true:

$$b_1 - q - \frac{e^{-a_2 t}}{a_2} (a_2 - a_1)(m_c - q)^{1 - \frac{a_2}{a_1}} (m_0 - q)^{\frac{a_2}{a_1}} - \frac{a_1(b_2 - q)}{a_2} > \quad (46)$$

$$b_1 - q - \frac{e^{-a_2 t_c}}{a_2} (a_2 - a_1)(m_c - q)^{1 - \frac{a_2}{a_1}} (m_0 - q)^{\frac{a_2}{a_1}} - \frac{a_1(b_2 - q)}{a_2} \quad (47)$$

Here we substitute  $t_c$  in Eq. 47 with Eq. 31 and we get:

$$b_1 - q - \frac{(a_2 - a_1)(m_c - q)}{a_2} - \frac{a_1(b_2 - q)}{a_2} = \quad (48)$$

$$a_1 \left( \frac{b_1 - m_c}{a_1} - \frac{b_2 - m_c}{a_2} \right) = a_1(n_c - n_c) = 0 \quad (49)$$

Hence, we have:

$$b_1 - q - \frac{e^{-a_2 t}}{a_2} (a_2 - a_1)(m_c - q)^{1 - \frac{a_2}{a_1}} (m_0 - q)^{\frac{a_2}{a_1}} - \frac{a_1(b_2 - q)}{a_2} > 0 \quad (50)$$

And the second derivative of TTS over the disruption vehicle accumulation  $n'$  is positive.  $\square$

#### 4.2. Supply disruption

While a positive second derivative of time spent on traffic demand signifies the fragility of the road transportation network to demand disruptions, establishing a positive second derivative of time spent concerning the magnitude of MFD disruption would demonstrate the fragility from the perspective of supply disruptions. Here we use a supply disruption magnitude coefficient  $r$  and the disrupted MFD is expressed as  $(1-r)G(n)$ . Although real-world MFD may be decreased in various shapes, we use this simple approach as applied in Ambühl et al. (2020) when studying the uncertainties of MFDs. The physical meaning of  $(1-r)G(n)$  relates to the decrease of the free-flow speed, for instance, due to snowy weather and icy roads, while the maximal density of the network remains unchanged. The traffic demand at equilibrium before the MFD disruption is  $q = G(k_0)$ , or  $q = G(n_0)$ . After the supply disruption, as per Assumption 2, the supply disruption magnitude coefficient  $r$  is not significantly large so the traffic demand remains below the maximal capacity on the disrupted MFD profile, and the new equilibrium point is  $q = (1-r)G(k'(r))$ , or  $q = (1-r)G(n'(r))$ . It should be noted that, unlike the study of demand disruption, when studying supply disruptions,  $k'(r)$  is a dependent variable on  $r$ .

##### 4.2.1. Onset of supply disruption on the microscopic level

First, we study the fragile property of the road transportation networks under the onset of supply disruptions based on the microscopic model Greenshields FD.

**Proposition 4.** *Road transportation systems are fragile with the onset of supply disruptions on the microscopic level.*

*Proof.* The base demand  $q$  is constant before and after the onset of the supply disruption.

$$q = G(k_0) = (1-r)G(k'(r)) = (1-r)(ak'(r)^2 + bk'(r)) \quad (51)$$

So, the traffic density of the new equilibrium point after the MFD disruption would be:

$$k'(r) = \frac{\sqrt{b^2 + \frac{4aq}{1-r}} - b}{2a} \quad (52)$$

The  $ATS$  and its first and second derivatives are:

$$ATS = \frac{L}{v(k')} = \frac{Lk'(r)}{q} = \frac{L}{2aq} \left( (b^2 + \frac{4aq}{1-r})^{\frac{1}{2}} - b \right) \quad (53)$$

$$\frac{dATS}{dr} = L(b^2(1-r) + 4aq)^{-\frac{1}{2}}(1-r)^{-\frac{3}{2}} \quad (54)$$

$$\frac{d^2ATS}{dr^2} = \frac{b^2L}{2}(b^2(1-r) + 4aq)^{-\frac{3}{2}}(1-r)^{-\frac{3}{2}} + \frac{3L}{2}(b^2(1-r) + 4aq)^{-\frac{1}{2}}(1-r)^{-\frac{5}{2}} \quad (55)$$

As  $k'$  has a physical meaning of density after disruption, hence, it should have real roots with  $b^2 + \frac{4aq}{1-r}$  being positive. And since  $1-r$  needs to be positive as well, therefore,  $\frac{d^2ATS}{dr^2}$  is always positive and indicates the fragility property of transportation networks when faced with supply disruption on the microscopic level. Likewise to the proof of demand disruption, the Daganzo FD is a special case of the MoC, so we directly prove the fragility on the macroscopic level with MoC. □

#### 4.2.2. Onset of supply disruption on the macroscopic level

Since the proof of fragility under supply disruption with Geroliminis MFD involves solving the roots for cubic equations. For simplicity reasons, we prove only With Daganzo MoC, and we have the traffic demand  $q$  and the traffic density of the new equilibrium  $k$  as:

**Proposition 5.** *Road transportation systems are fragile with the onset of supply disruptions on the macroscopic level.*

*Proof.*

$$q = (1-r)(uk'(r) + c) \quad (56)$$

$$k'(r) = \frac{\frac{q}{1-r} - c}{u} \quad (57)$$

The  $ATS$  and its first and second derivatives are:

$$ATS = \frac{Lk'(r)}{q} = \frac{L}{qu} \left( \frac{q}{1-r} - c \right) \quad (58)$$

$$\frac{dATS}{dr} = \frac{L}{u}(1-r)^{-2} \quad (59)$$

$$\frac{d^2ATS}{dr^2} = \frac{2L}{u}(1-r)^{-3} \quad (60)$$

As per Assumption 1, when studying supply disruptions, we focus on the uncongested zone of the MFD, meaning the slope of these relevant cuts is positive so that both the first and second derivatives are positive. □

#### 4.2.3. Recovery from supply disruption

To study the possible fragile properties of road transportation networks regarding the recovery process from supply disruptions, we need to combine the conclusions from Sections 4.1.3 and 4.2.2. In Section 4.1.3, we've proven the recovery process to be either fragile when the traffic state shifts from the more congested branch to the less congested branch for any two consecutive cuts on the Daganzo MFD, or to be neither fragile nor antifragile when it stays only on one single branch. Therefore, it can be mathematically summarized as  $\frac{d^2 TTS}{dn'^2} \geq 0$ . Likewise to the proof of positive second derivative, with the assumption of  $a_1 > 0$  as the branch is below the critical density following Assumption 1, we can easily prove the first derivative  $\frac{dTTS}{dn'}$  to be non-negative as well with Eq. 34 and Eq. 40. For the proof of recovery from supply disruptions, as shown in Figure 8, similar to Section 4.2.2, the relationship between the original and new equilibrium points before and after MFD disruptions can be expressed as:

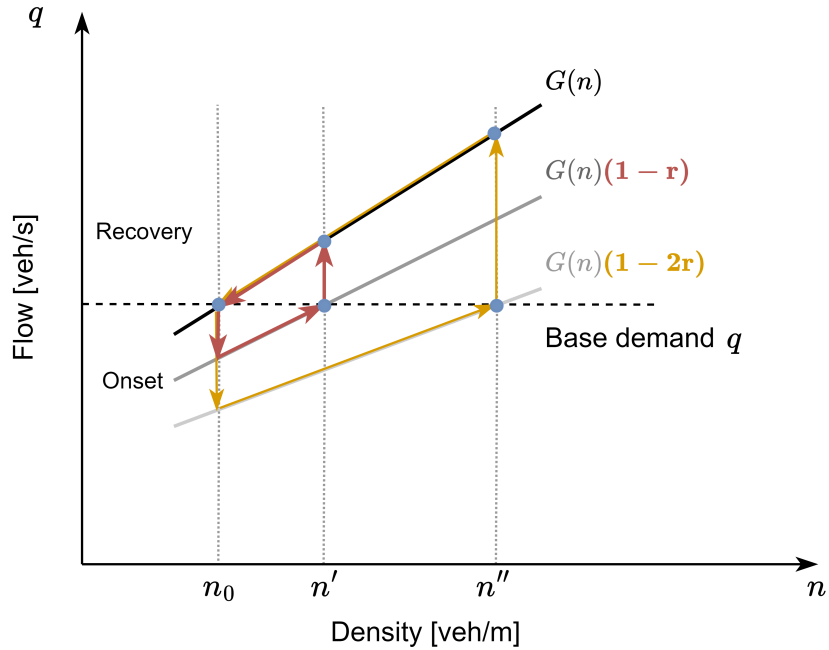


Figure 8: Recovery from supply disruption

**Proposition 6.** *Road transportation systems are fragile when going through the recovery process from supply disruptions.*

*Proof.*

$$q = un_0 + c = (1 - r)(un' + c) \quad (61)$$

$$n'(r) = \frac{un_0 + c}{u(1 - r)} - c/u \quad (62)$$

The first and second derivatives of  $n'$  over the supply disruption magnitude coefficient  $r$  are:

$$\frac{dn'}{dr} = \frac{un_0 + c}{u}(1 - r)^{-2} \quad (63)$$

$$\frac{d^2n'}{dr^2} = \frac{2(un_0 + c)}{u}(1 - r)^{-3} \quad (64)$$

Since  $u$  and  $un_0 + c$  are both positive, therefore, the first and second derivatives of  $n'$  over  $r$  are positive as well. Additionally, it can be easily proven that when considering the transition from a more congested to a less congested branch, the same conclusion also holds. As  $TTS$  is a function of  $n'$  and  $n'$  is again a function of  $r$ , by applying the chain rule, we can get the second derivative of  $TTS$  over  $r$ :

$$\frac{d^2TTS}{dr^2} = \frac{d}{dr} \left( \frac{dTTS}{dn'} \cdot \frac{dn'}{dr} \right) \quad (65)$$

$$= \frac{d^2TTS}{dn_0'^2} \cdot \left( \frac{dn'}{dr} \right)^2 + \frac{dTTS}{dn'} \cdot \frac{d^2n'}{dr^2} \quad (66)$$

Since all the four components of the Eq. 66 have been proven to be non-negative. Hence  $\frac{d^2TTS}{dr^2}$  is also non-negative and we've proven the fragile nature of road transportation systems regarding the recovery process of supply disruptions. □

## 5. Numerical simulation

Although researchers always consider MFDs to be well-defined, in the real world, road transportation systems and their MFDs are always subject to uncertainties all the time, as shown in Geroliminis and Daganzo (2008) and in Ambühl et al. (2021) with loop detector data over a year. This uncertainty cannot be reflected in the mathematical analysis, therefore, it is indispensable to show the influence of realistic stochasticity on the performance of transportation systems. Whether the system still maintains the fragile property under real-world uncertainties in MFD.

In this section, we simulate a congestion dissipation process. The MFD of the studied region is created by applying MoC in Daganzo and Geroliminis (2008) with realistic parameters in the city center of Zurich. Some parameters, e.g., free-flow speed, back-propagation speed, maximal density, and capacity are provided in Ambühl et al. (2020) for Zurich with queried routes in Google API and with other validation methods. The total and average lane length for District 1 is queried through SUMO with OpenStreetMap API. The average trip length in the city of Zurich is studied in Schüssler and Axhausen (2008). We introduce stochasticity in District 1 of Zurich with real traffic light data, which is readily available in Genser et al. (2023). Since the signalization in Zurich is actuated based on the present traffic flow, they do not strictly follow a fixed-time signal cycle. Despite this actuation, a concentrated distribution can be easily observed in the dataset and we assume the green split of the cycle follows a normal distribution. The offset is considered to be zero in a way similar to the actuated signal in Yokohama in Daganzo and Geroliminis (2008). The parameters are summarized in Tab. 2.

As the average green time of the signal is 14.8 s and its standard deviation is 2.5 s, following the procedure described in Daganzo and Geroliminis (2008), we can produce three groups of cuts with green time being  $\mu_G - \sigma_G$ ,  $\mu_G$ , or  $\mu_G + \sigma_G$ , and each group of cuts contains at least three cuts, as Fig. 9 shows. The group of cuts with a longer green time of signalization yields a greater MFD, and vice versa. The MFDs share the same maximal vehicle accumulation at around 10000 vehicles.

Now we start the numerical simulation with different initial disruption demands  $n_0$  from 1000 to 8000 vehicles with a step size of 500 vehicles. The simulation time is the same 5000 seconds for each scenario with a different initial demand. Fig. 10(a) demonstrates that TTS grows

Table 2: Estimated parameters for the city center of Zurich

Parameters	Notation	Unit	Value
Free-flow speed	$u_0$	m/s	12.5
Back-propagation speed	$w_0$	m/s	6.0
Maximal density	$\kappa$	veh/m	0.145
Capacity	$s$	veh/s	0.51
Total lane length	$D$	m	68631
Average lane length	$l$	m	167
Average trip length	$L$	m	7110
Signal cycle time	$C$	s	50
Signal green time (mean)	$\mu_G$	s	14.8
Signal green time (std.)	$\sigma_G$	s	2.5
Offset	$\delta$	s	0

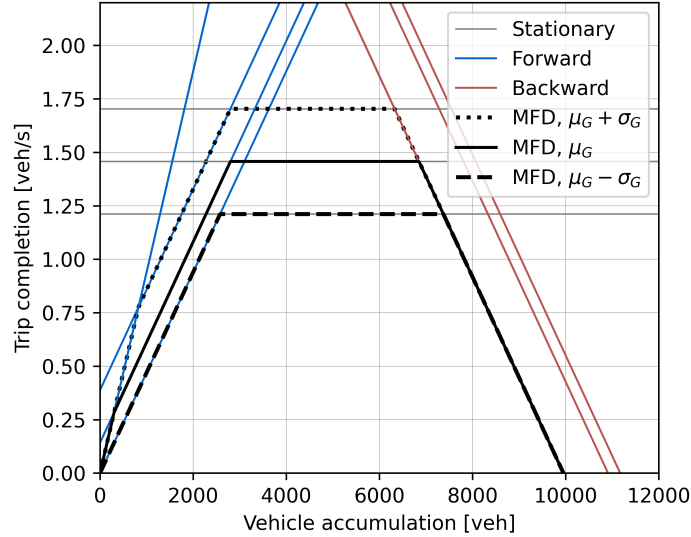
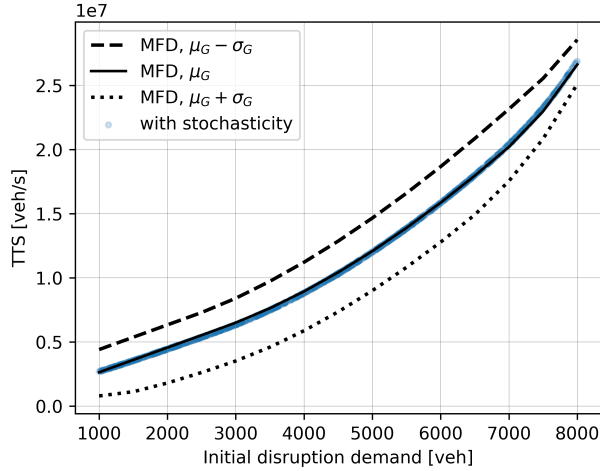


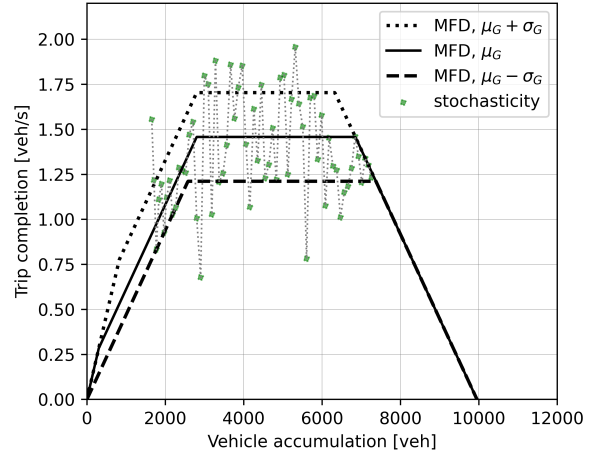
Figure 9: The MFD of the city center of Zurich through MoC

exponentially with linearly increasing initial disruption demand. The solid, dashed, or dotted line each represents a deterministic MFD calculated with a signal green time being  $\mu_G$ ,  $\mu_G - \sigma_G$ , or  $\mu_G + \sigma_G$ . Other than these three lines, there are also 500 scattering points forming the blue curve. Each scatter point is composed of a full congestion dissipation process sampled with equal intervals between an initial traffic demand varying from 1000 vehicles to 8000 vehicles. At each time step, a stochastic signal green time is chosen following the normal distribution  $G \sim N(14.8, 2.5)$  based on real-world data, leading to an uncertain MFD profile as Fig. 10(b) shows. This is an example of how the congestion is dissipated in this urban road network, the green scattering points are sampled from every 80th point from 5000 timesteps in total.

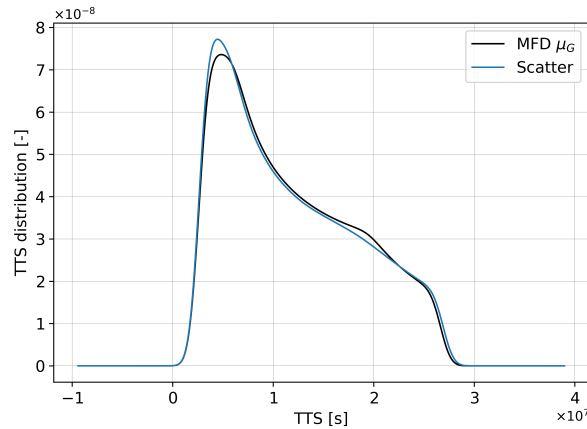
Since the scattering points closely align with the solid curve, it can be inferred that the influence of realistic stochasticity on the MFD is mostly negligible. However, an intriguing observation is that, when the disruption demand is relatively low, the blue curve dips slightly below the MFD of the solid curve. However, it appears to exceed the TTS of the MFD when the



(a) Demand disruption in the real world



(b) Stochasticity on the MFD



(c) TTS distribution w/o stochasticity

Figure 10: Numerical simulation with stochasticity

demand is substantial. When we show the distribution of these two curves, as in Fig. 10(c), the curve made from scatter points has a more concentrated distribution at lower TTS while having a greater distribution at higher TTS, indicating a more left-skewed distribution compared to the distribution of TTS without realistic stochasticity. This can also be demonstrated by calculating the skewness of these two curves. When there is no stochasticity, the skewness is 0.50 while the skewness for the curve with stochasticity has a value of 0.53. A greater skewness indicates a more fragile system, which means that by introducing realistic stochasticity, the urban road network becomes even more fragile.

## 6. Conclusion

This research systematically demonstrated the fragile nature of road transportation systems with rigorous mathematical analysis and numerical simulation under realistic stochasticity. The mathematical proof comprehends the study of fragility under 1) microscopic - macroscopic, 2) demand disruption - supply disruption, and 3) onset of disruption - recovery from disruption.

With essential assumptions regarding the disruption density in comparison to the critical density as well as the base traffic demand, we've validated the fragility of road transportation systems from various perspectives. Furthermore, through a numerical simulation with realistic data, we concluded that real-world stochasticity has a limited impact on the fragile characteristics of the system but contributes to rendering the system even more fragile. Lately, researchers have explored the potential utilization of MFD in railway operations (Corman et al., 2019) and in aviation (Safadi et al., 2023). The fragility observed in urban road networks may be extended to various transportation systems. This study aims to offer insights to researchers, emphasizing the fragile characteristics of transportation systems and encouraging the design of antifragile traffic control strategies in the future.

## References

- Ambühl, L., Loder, A., Bliemer, M.C., Menendez, M., Axhausen, K.W., 2020. A functional form with a physical meaning for the macroscopic fundamental diagram. *Transportation Research Part B: Methodological* 137, 119–132. URL: <https://linkinghub.elsevier.com/retrieve/pii/S0191261517310123>, doi:10.1016/j.trb.2018.10.013.
- Ambühl, L., Loder, A., Leclercq, L., Menendez, M., 2021. Disentangling the city traffic rhythms: A longitudinal analysis of MFD patterns over a year. *Transportation Research Part C: Emerging Technologies* 126, 103065. URL: <https://www.sciencedirect.com/science/article/pii/S0968090X21000917>, doi:10.1016/j.trc.2021.103065.
- Axenie, C., Kurz, D., Saveriano, M., 2022. Antifragile Control Systems: The Case of an Anti-Symmetric Network Model of the Tumor-Immune-Drug Interactions. *Symmetry* 14, 2034. doi:10.3390/sym14102034.
- Axenie, C., Saveriano, M., 2023. Antifragile Control Systems: The case of mobile robot trajectory tracking in the presence of uncertainty.
- Büchel, B., Marra, A.D., Corman, F., 2022. COVID-19 as a window of opportunity for cycling: Evidence from the first wave. *Transport Policy* 116, 144–156. URL: <https://www.sciencedirect.com/science/article/pii/S0967070X21003565>, doi:10.1016/j.tranpol.2021.12.003.
- Calvert, S.C., Snelder, M., 2018. A methodology for road traffic resilience analysis and review of related concepts. *Transportmetrica A: Transport Science* 14, 130–154. URL: <https://doi.org/10.1080/23249935.2017.1363315>, doi:10.1080/23249935.2017.1363315. publisher: Taylor & Francis eprint: <https://doi.org/10.1080/23249935.2017.1363315>.
- Chang, G.L., Xiang, H., 2003. The relationship between congestion levels and accidents URL: <https://trid.trb.org/view/680981>. number: MD-03-SP 208B46,.
- Chen, C., Huang, Y.P., Lam, W.H.K., Pan, T.L., Hsu, S.C., Sumalee, A., Zhong, R.X., 2022. Data efficient reinforcement learning and adaptive optimal perimeter control of network traffic dynamics. *Transportation Research Part C: Emerging Technologies* 142, 103759. doi:10.1016/j.trc.2022.103759.

- Ciuffini, F., Tengattini, S., Bigazzi, A.Y., 2023. Mitigating Increased Driving after the COVID-19 Pandemic: An Analysis on Mode Share, Travel Demand, and Public Transport Capacity. *Transportation Research Record* 2677, 154–167. URL: <https://doi.org/10.1177/03611981211037884>, doi:10.1177/03611981211037884. publisher: SAGE Publications Inc.
- Coppitters, D., Contino, F., 2023. Optimizing upside variability and antifragility in renewable energy system design. *Scientific Reports* 13, 9138. URL: <https://www.nature.com/articles/s41598-023-36379-8>, doi:10.1038/s41598-023-36379-8. number: 1 Publisher: Nature Publishing Group.
- Corman, F., Henken, J., Keyvan-Ekbatani, M., 2019. Macroscopic fundamental diagrams for train operations - are we there yet?, in: *2019 6th International Conference on Models and Technologies for Intelligent Transportation Systems (MT-ITS)*, pp. 1–8. URL: <https://ieeexplore.ieee.org/abstract/document/8883374>, doi:10.1109/MTITS.2019.8883374.
- Corman, F., Quaglietta, E., Goverde, R.M.P., 2018. Automated real-time railway traffic control: an experimental analysis of reliability, resilience and robustness. *Transportation Planning and Technology* 41, 421–447. URL: <https://doi.org/10.1080/03081060.2018.1453916>, doi:10.1080/03081060.2018.1453916. publisher: Routledge eprint: <https://doi.org/10.1080/03081060.2018.1453916>.
- Daganzo, C.F., 1994. The cell transmission model: A dynamic representation of highway traffic consistent with the hydrodynamic theory. *Transportation Research Part B: Methodological* 28, 269–287. URL: <https://www.sciencedirect.com/science/article/pii/0191261594900027>, doi:10.1016/0191-2615(94)90002-7.
- Daganzo, C.F., Geroliminis, N., 2008. An analytical approximation for the macroscopic fundamental diagram of urban traffic. *Transportation Research Part B: Methodological* 42, 771–781. URL: <https://www.sciencedirect.com/science/article/pii/S0191261508000799>, doi:10.1016/j.trb.2008.06.008.
- Daganzo, C.F., Lehe, L.J., Argote-Cabanero, J., 2018. Adaptive offsets for signalized streets. *Transportation Research Part B: Methodological* 117, 926–934. URL: <https://linkinghub.elsevier.com/retrieve/pii/S0191261517306914>, doi:10.1016/j.trb.2017.08.011.
- Duan, Y., Lu, F., 2014. Robustness of city road networks at different granularities. *Physica A: Statistical Mechanics and its Applications* 411, 21–34. URL: <https://www.sciencedirect.com/science/article/pii/S037843711400466X>, doi:10.1016/j.physa.2014.05.073.
- Federal Statistical Office of Switzerland, 2020. *Mobilität und Verkehr: Panorama - 2020 | Publikation*. URL: <https://www.bfs.admin.ch/asset/de/13695321>.
- Genser, A., Kouvelas, A., 2022. Dynamic optimal congestion pricing in multi-region urban networks by application of a Multi-Layer-Neural network. *Transportation Research Part C: Emerging Technologies* 134, 103485. URL: <https://www.sciencedirect.com/science/article/pii/S0968090X2100471X>, doi:10.1016/j.trc.2021.103485.
- Genser, A., Makridis, M.A., Yang, K., Abmühl, L., Menendez, M., Kouvelas, A., 2023. A traffic signal and loop detector dataset of an urban intersection regulated by a fully actuated signal

- control system. Data in Brief 48, 109117. URL: <https://www.sciencedirect.com/science/article/pii/S2352340923002366>, doi:10.1016/j.dib.2023.109117.
- Geroliminis, N., Daganzo, C.F., 2008. Existence of urban-scale macroscopic fundamental diagrams: Some experimental findings. *Transportation Research Part B: Methodological* 42, 759–770. URL: <https://www.sciencedirect.com/science/article/pii/S0191261508000180>, doi:10.1016/j.trb.2008.02.002.
- Geroliminis, N., Haddad, J., Ramezani, M., 2013. Optimal Perimeter Control for Two Urban Regions With Macroscopic Fundamental Diagrams: A Model Predictive Approach. *IEEE Transactions on Intelligent Transportation Systems* 14, 348–359. doi:10.1109/TITS.2012.2216877. conference Name: IEEE Transactions on Intelligent Transportation Systems.
- Greenshields, B.D., Thompson, J.T., Dickinson, H.C., Swinton, R.S., 1934. The photographic method of studying traffic behavior. *Highway Research Board Proceedings* 13. URL: <https://trid.trb.org/view/120821>.
- Jensen, J.L.W.V., 1906. Sur les fonctions convexes et les inégalités entre les valeurs Moyennes URL: <https://zenodo.org/records/2371297>, doi:10.1007/bf02418571.
- Kim, H., Muñoz, S., Osuna, P., Gershenson, C., 2020. Antifragility Predicts the Robustness and Evolvability of Biological Networks through Multi-Class Classification with a Convolutional Neural Network. *Entropy* 22, 986. doi:10.3390/e22090986.
- Kouvelas, A., Saeedmanesh, M., Geroliminis, N., 2017. Enhancing model-based feedback perimeter control with data-driven online adaptive optimization. *Transportation Research Part B: Methodological* 96, 26–45. URL: <https://www.sciencedirect.com/science/article/pii/S019126151630710X>, doi:10.1016/j.trb.2016.10.011.
- Leclercq, L., Geroliminis, N., 2013. Estimating MFDs in simple networks with route choice. *Transportation Research Part B: Methodological* 57, 468–484. URL: <https://linkinghub.elsevier.com/retrieve/pii/S0191261513000878>, doi:10.1016/j.trb.2013.05.005.
- Manso, G., Balsmeier, B., Fleming, L., 2020. Heterogeneous Innovation and the Antifragile Economy .
- Mattsson, L.G., Jenelius, E., 2015. Vulnerability and resilience of transport systems – A discussion of recent research. *Transportation Research Part A: Policy and Practice* 81, 16–34. URL: <https://www.sciencedirect.com/science/article/pii/S0965856415001603>, doi:10.1016/j.tra.2015.06.002.
- Rodrigues, F., Azevedo, C.L., 2019. Towards Robust Deep Reinforcement Learning for Traffic Signal Control: Demand Surges, Incidents and Sensor Failures, in: 2019 IEEE Intelligent Transportation Systems Conference (ITSC), pp. 3559–3566. doi:10.1109/ITSC.2019.8917451.
- Ruel, J.J., Ayres, M.P., Ruel, J.J., Ayres, M.P., 1999. Jensen’s inequality predicts effects of environmental variation. *Trends in Ecology & Evolution* 14, 361–366. URL: [https://www.cell.com/trends/ecology-evolution/abstract/S0169-5347\(99\)01664-X](https://www.cell.com/trends/ecology-evolution/abstract/S0169-5347(99)01664-X), doi:10.1016/S0169-5347(99)01664-X. publisher: Elsevier.

- Safadi, Y., Fu, R., Quan, Q., Haddad, J., 2023. Macroscopic Fundamental Diagrams for Low-Altitude Air city Transport. *Transportation Research Part C: Emerging Technologies* 152, 104141. URL: <https://www.sciencedirect.com/science/article/pii/S0968090X23001304>, doi:10.1016/j.trc.2023.104141.
- Saidi, S., Koutsopoulos, H.N., Wilson, N.H.M., Zhao, J., 2023. Train following model for urban rail transit performance analysis. *Transportation Research Part C: Emerging Technologies* 148, 104037. URL: <https://www.sciencedirect.com/science/article/pii/S0968090X23000268>, doi:10.1016/j.trc.2023.104037.
- Schüssler, N., Axhausen, K.W., 2008. Identifying trips and activities and their characteristics from gps raw data without further information. *Arbeitsberichte Verkehrs-und Raumplanung* 502.
- Shang, W.L., Gao, Z., Daina, N., Zhang, H., Long, Y., Guo, Z., Ochieng, W.Y., 2022. Benchmark Analysis for Robustness of Multi-Scale Urban Road Networks Under Global Disruptions. *IEEE Transactions on Intelligent Transportation Systems*, 1–11 URL: <https://ieeexplore.ieee.org/abstract/document/9714769>, doi:10.1109/TITS.2022.3149969. conference Name: IEEE Transactions on Intelligent Transportation Systems.
- Taleb, N.N., 2012. *Antifragile: Things That Gain from Disorder*. Reprint edition ed., Random House Publishing Group, New York.
- Taleb, N.N., Douady, R., 2013. Mathematical definition, mapping, and detection of (anti)fragility. *Quantitative Finance* 13, 1677–1689. doi:10.1080/14697688.2013.800219.
- U.S. Bureau of Public Roads, 1964. *Traffic assignment manual for application with a large, high speed computer*. US Department of Commerce.
- U.S. Congress, Office of Technology Assessment, 1984. *Airport system development*. U.S. Government Printing Office. Google-Books-ID: hihBG2mzB1MC.
- U.S. Department of Transportation, 2019. *National Transportation Statistics (NTS)* URL: <https://tinyurl.com/rosapntlbtSNTS>, doi:10.21949/1503663. publisher: Not Available.
- Zhang, R., Zhang, J., 2021. Long-term pathways to deep decarbonization of the transport sector in the post-COVID world. *Transport Policy* 110, 28–36. URL: <https://www.sciencedirect.com/science/article/pii/S0967070X21001621>, doi:10.1016/j.tranpol.2021.05.018.
- Zhou, D., Gayah, V.V., 2021. Model-free perimeter metering control for two-region urban networks using deep reinforcement learning. *Transportation Research Part C: Emerging Technologies* 124, 102949. URL: <https://linkinghub.elsevier.com/retrieve/pii/S0968090X20308469>, doi:10.1016/j.trc.2020.102949.
- Zhou, Y., Wang, J., Yang, H., 2019. Resilience of Transportation Systems: Concepts and Comprehensive Review. *IEEE Transactions on Intelligent Transportation Systems* 20, 4262–4276. doi:10.1109/TITS.2018.2883766. conference Name: IEEE Transactions on Intelligent Transportation Systems.